Cell Reports, Volume *36*

Supplemental information

Hemozoin-mediated inflammasome activation limits long-lived anti-malarial immunity

Angela D. Pack, Patrick V. Schwartzhoff, Zeb R. Zacharias, Daniel Fernandez-Ruiz, William R. Heath, Prajwal Gurung, Kevin L. Legge, Chris J. Janse, and Noah S. Butler

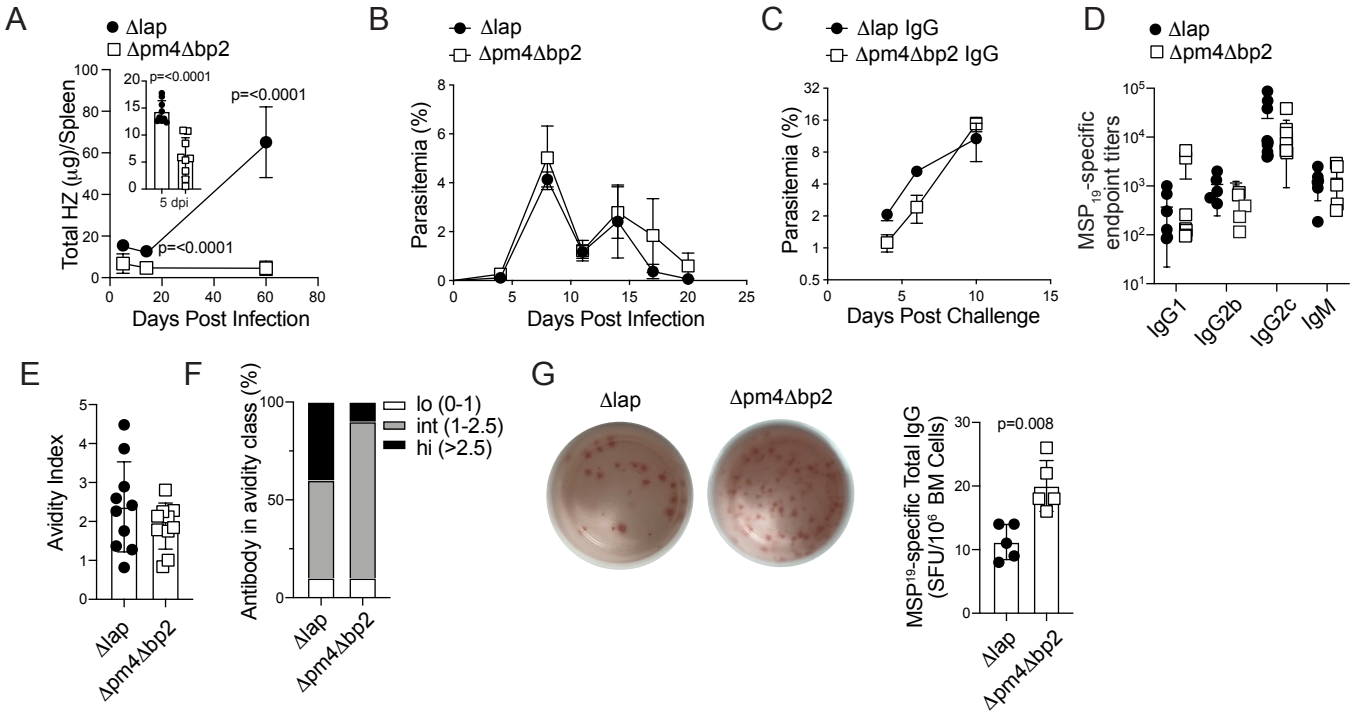

Supplemental Figure 1. Growth and clearance kinetics of Δpm4Δbp2 and Δlap parasites and total parasite-specific antibody titers during primary infection (Related to Figure 1)
(A) Quantification of hemozoin abundance in spleen of mice following primary infection with Δpm4Δbp2 and Δlap parasites. (B) Kinetics of circulating parasite burden during primary infection with Δpm4Δbp2 and Δlap parasites. (C) Kinetics of circulating parasite burden during virulent *Pb* ANKA challenge of naïve mice receiving purified IgG from Δpm4Δbp2 and Δlap immune donors. (D) MSP119-specific endpoint titers at approximately 60 days p.i. (E) Avidity index, determined by the amount (M) of NH_4SCN needed to elute $MSP1_{1\text{-}19}$-specific antibodies and percentage of antibodies per class (lo,int,hi) (F). (G) Representative images and summary of $MSP1_{1\text{-}19}$-specific ELISPOT of bone marrow PCs on day 60 following infection with mutant parasites. Data (Mean +/- S.E.M) in panel B are summary of 3 experiments with n=4-6. Data (Mean +/- S.D.) in panels A,C and D-F are summary from 2 independent experiments. Data (Mean +/- S.D.) in G are representative of 3 experiments with n=4-6.

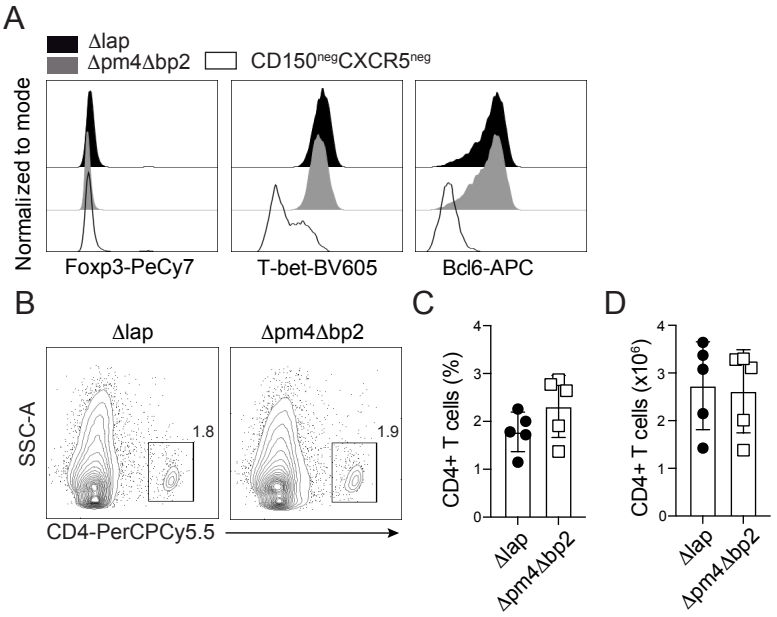

Supplemental Figure 2. Transcription factor expression and CD4 T cell engraftment in Tcrα-/- recipients (Related to Figure 3) (A) Representative histograms of Foxp3, T-bet, and Bcl-6 expression in polyclonal CXCR5^{hi}PD-1^{hi} GC TFH (14 dpi) shown in figure 3I. Relative gMFI was calculated by dividing the gMFI of each transcription factor within the GC TFH population by that of the CD150^{neg}CXCR5^{neg} CD4 population within each respective sample. CD150^{lo}CXCR5^{int} CD4+ T cells were sorted from mice infected with Δpm4Δbp2 and Δlap parasites (d7) and were transferred to Tcrα-/- recipients (B) Representative flow plots defining CD4+T cells collected from Tcrα-/- recipients 14 days after infection with either Δpm4Δbp2 or Δlap parasites. Frequency (C) and number (D) of CD4 positive T cells within the total lymphocyte gate in the spleens of Tcrα-/- mice receiving CD150^{lo}CXCR5^{int} CD4+ T cells from either Δpm4Δbp2 or Δlap infected donor mice. Data (Mean +/- S.D.) are representative of 2 independent experiments with n=4-5.

Supplemental Figure 3. Pack et al. 2021

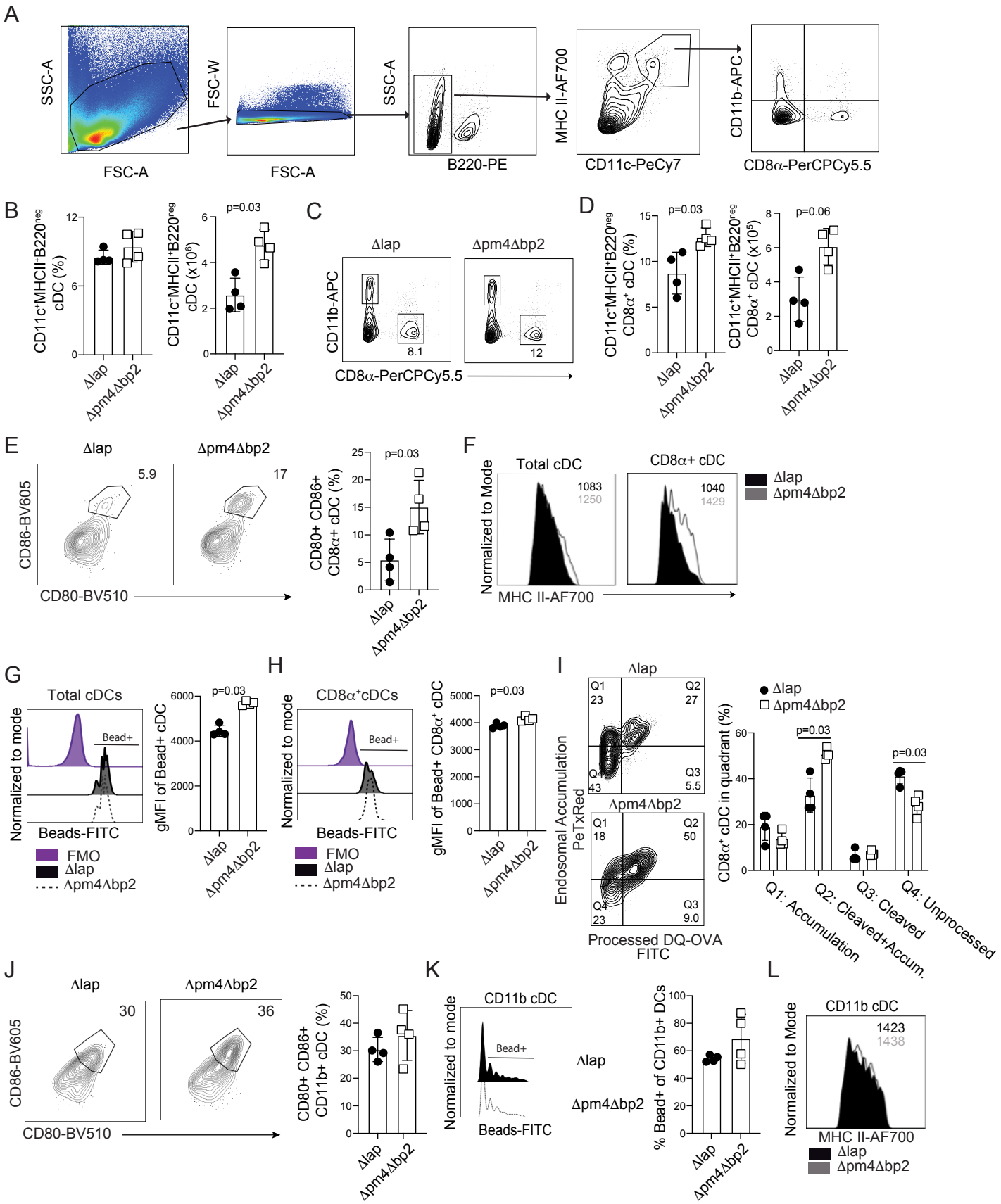

Supplemental Figure 3. Representative cDC1 and cDC2 gating, CD80 and CD86 expression and impacts of hemozoin on cDC2 phenotype and function (Related to Figure 4)
(A) Gating strategy for identification of total ($CD11c^{+}MHCII^{+}B220^{neg}$) conventional dendritic cells (cDC), cDC2 ($CD11b^{+}CD8\alpha^{neg}$) and cDC1 ($CD11b^{neg}CD8\alpha^{+}$). C57BL/6 mice were infected with either Δpm4Δbp2 or Δlap parasites and spleens were harvested on day 10 p.i. and DC were liberated by digestion as described in Methods.
Frequency and number of total $CD11c^{+}MHCII^{+}B220^{neg}$ conventional DC (B) and $CD11b^{neg}CD8\alpha^{+}$ cDC1 (C,D).
(E) CD80 and CD86 expression on $CD11b^{neg}CD8\alpha^{+}$ cDC1 on day 10 p.i. (F) MHC II expression on total and $CD11b^{neg}CD8\alpha^{+}$ cDC1. Histogram and summary graphs of bead positive total (G) and $CD11b^{neg}CD8\alpha$+ cDC1 (H) recovered from Δlap (shaded), Δpm4Δbp2-infected mice (dotted), control (no-beads) (shaded purple).
(I) Flow plots and summary data of DQ-OVA protein processing assay with $CD11b^{neg}CD8\alpha^{+}$ cDC.
CD80 and CD86 expression (J) on $CD11b^{+}CD8\alpha^{neg}$ cDC2 on day 10 p.i. (K) In vitro fluorescent bead phagocytosis by $CD11b^{+}CD8\alpha^{neg}$ cDC2 on day 10 p.i. (L) MHC II expression on $CD11b^{+}CD8\alpha^{neg}$ cDC2. All presented data (Mean +/- S.D.) are representative of 4 independent experiments with n=4-5.

Supplemental Figure 4. Pack et al. 2021

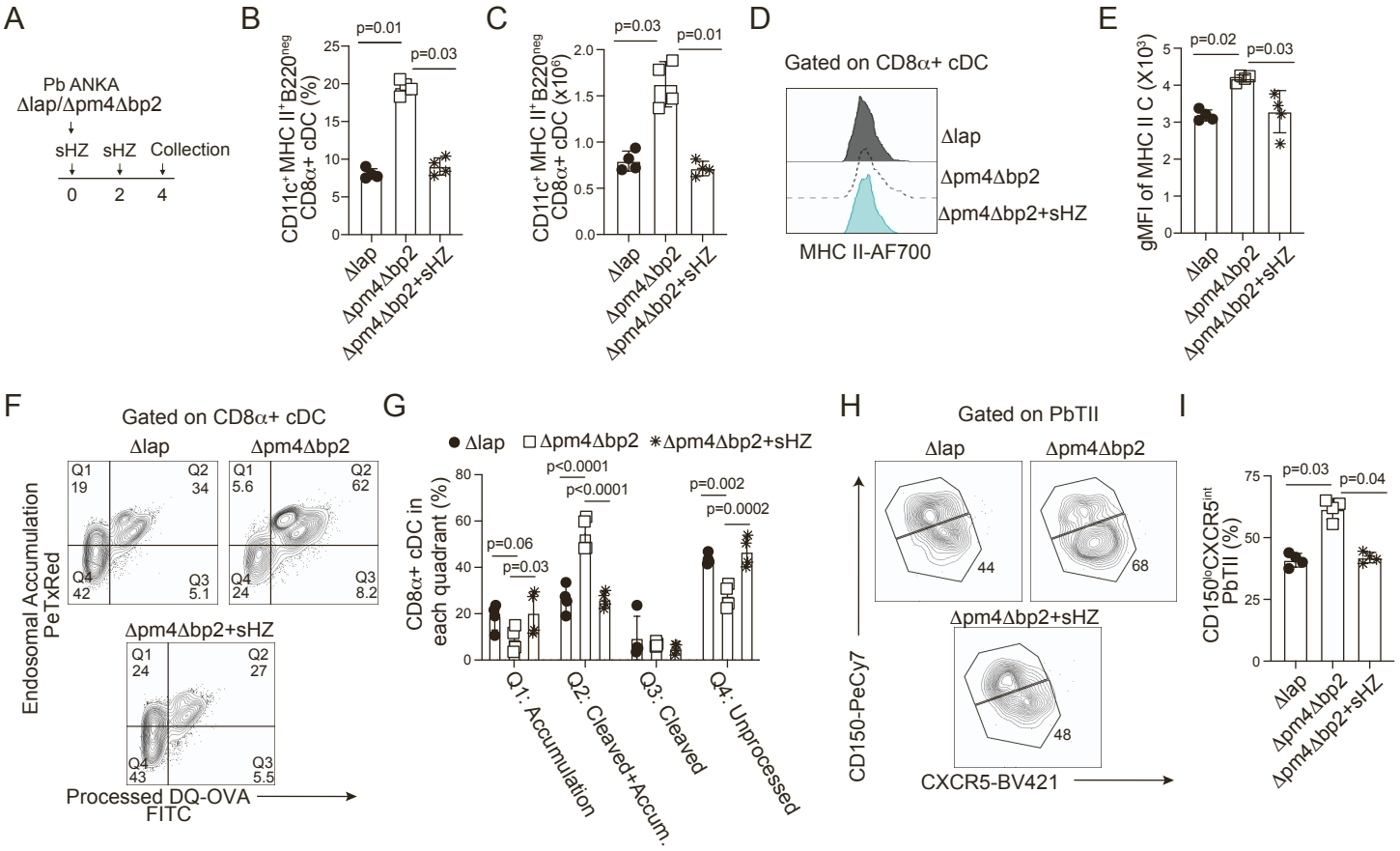

Supplemental Figure 4. Injection of synthetic hemozoin compromises cDC1 and alters T_{FH} differentiation (Related to Figure 5) (A) WT mice were infected with Δlap or Δpm4Δbp2 parasites and injected with PBS, while an additional group of Δpm4Δbp2-infected animals received injections of synthetic hemozoin (sHZ). Spleens were collected on day 4 of infection for analysis. Frequency and number (B,C) and representative histograms and summary graph of gMFI of MHC II expression (D,E) on $CD11b^{neg}CD8\alpha^{+}$ cDC1. (F,G) Flow plots and summary data of DQ-OVA protein processing assay. Representative plots (H) and frequency (I) of T_{FH} precursor ($CD150^{lo}CXCR5^{int}$) by day 4 p.i. All data (Mean +/- S.D.) are representative of two independent experiments with n=4 per group.

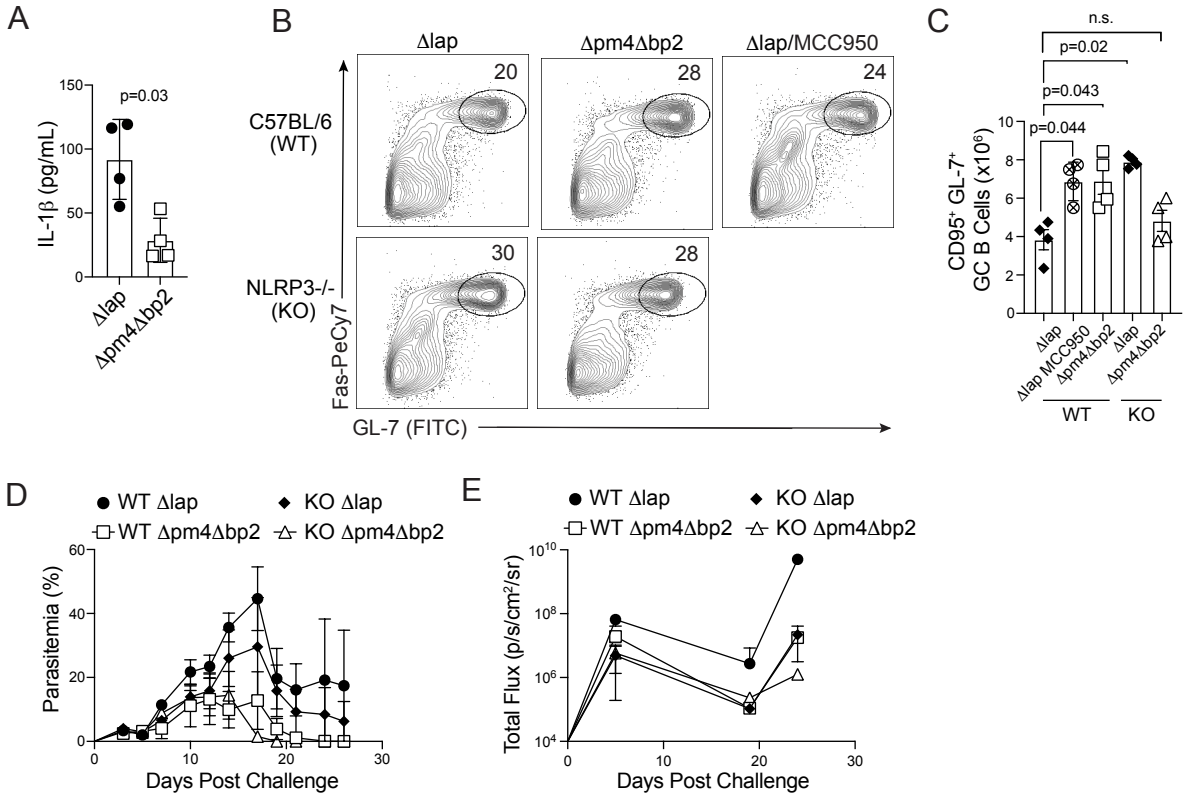

Supplemental Fig. 5. IL-1β in mutant *P. berghei*-infected WT mice and humoral immune responses and protection following *P. yoelii*-infection in WT and NLRP3$^{-/-}$ mice (Related to Figure 1C and Figure 6E-G)
(A) Serum IL-1β levels on day 10 p.i. following infection with Δlap and Δpm4Δbp2 parasites. Data are representative of two independent experiments. C57BL/6 (WT) and NLRP3$^{-/-}$ (KO) mice were infected with Δpm4Δbp2 and Δlap and WT mice were treated with MCC950 after Δlap infection. Representative flows (B) and frequency (C) of CD95^{+}GL-7^{+} GC B cells day 14 p.i. C57BL/6 and NLRP3$^{-/-}$ mice were immunized with Δpm4Δbp2 and Δlap parasites sixty days prior to challenge with a virulent *Pb* ANKA strain. Circulating (D) and total (E) parasite burden were quantified from mice used in Fig. 6E-G and Fig. 1C, respectively. Data (Mean +/- S.D.) in panels A-D are representative of two independent experiments with n=3-4 per experimental group. Data in panel E (Mean +/- S.E.M.) are summary data from two independent experiments and include luciferase imaging data from wild-type mice presented in Fig. 1C.

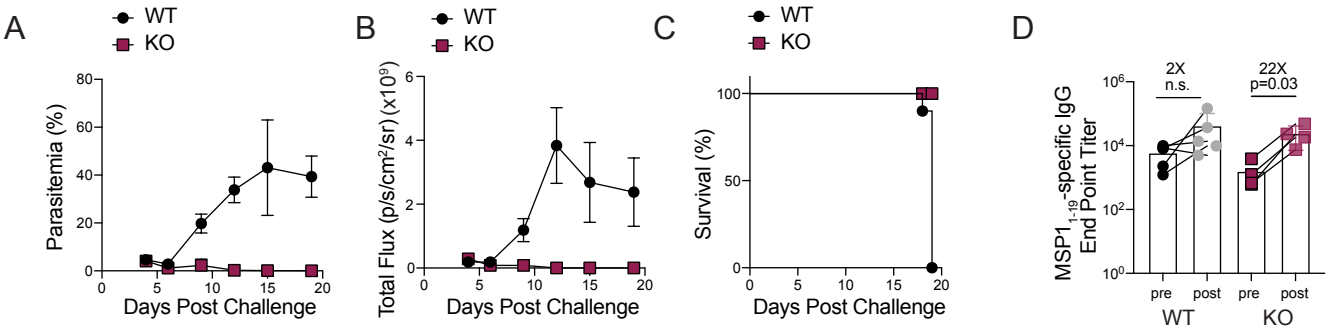

Supplemental Figure 6. Hemozoin compromises protective humoral immunity generated following *P. yoelii* 17XNL infection (Related to Figure 7) At approximately 50 days post immunization with *P. yoelli* 17XNL parasites, C57BL/6 (WT) and NLRP3$^{-/-}$ (KO) mice were challenged with a virulent *Pb* ANKA strain. Circulating (A) and total (B) parasite burden was quantified. (C) Frequency of immune mice that survived virulent *Pb*-ANKA challenge. (D) MSP1$_{1\text{-}19}$-specific IgG endpoint titers one day prior to (pre) and 5 days after (post) virulent *Pb*-ANKA challenge of *P. yoelii*-immune WT and NLRP3$^{-/-}$ mice. Data (Mean +/- S.D.) are representative of one experiment with n=5 per experimental group.